ACS Sustainable Chemistry & Engineering

Research Article

pubs.acs.org/journal/ascecg

Enhanced Formation of Stereocomplex Crystallites of High Molecular Weight Poly(L-lactide)/Poly(D-lactide) Blends from Melt by Using Poly(ethylene glycol)

Rui-Ying Bao, Wei Yang,* Xin-Feng Wei, Bang-Hu Xie, and Ming-Bo Yang

State Key Laboratory of Polymer Materials Engineering, College of Polymer Science and Engineering, Sichuan University, , Chengdu, 610065 Sichuan, China

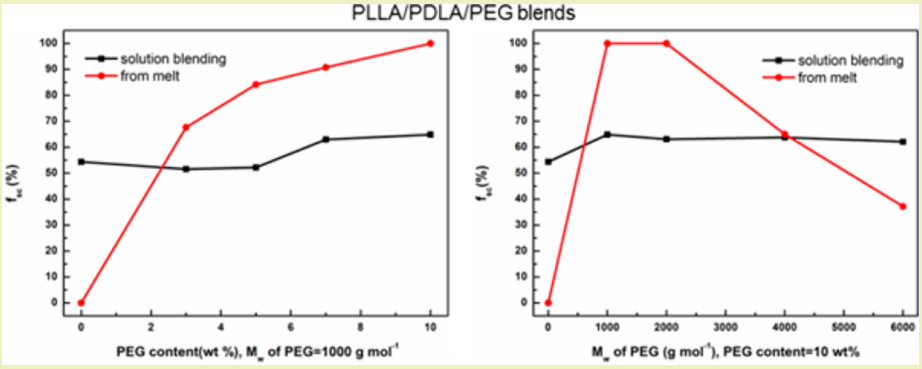

ABSTRACT: Melt processing of polymers is preferable in industry. Unfortunately, for high molecular weight (M_w) poly(L-lactide)/poly(D-lactide) (PLLA/PDLA) blends, exclusive formation of stereocomplex (sc) crystallites from the melt has never been achieved. We proposed a new and simple approach to enhance the melt crystallization of sc crystallites from high M_w PLLA/PDLA by using poly(ethylene glycol) (PEG). The crystallizability of the PLLA/PDLA blend is greatly enhanced by PEG during crystallization from the melt. The resulted crystalline structures depend on the M_w and content of PEG, and the crystallinity of sc crystallites increases with increasing content or decreasing M_w of PEG. More importantly, exclusive formation of sc crystallites is achieved in the blends with 10% PEG having M_w values of 1000 or 2000 g mol^{-1}. Polarized optical microscopy (POM) observation shows that the spherulitic growth rates of sc crystallites are accelerated. The results demonstrate that segmental mobility of polylactides (PLA) chains plays a dominant role on the formation of sc crystallites from melt and provide a simple way to prepare sc crystallites from high M_w PLA by melt blending and enlarge the applications of PLA.

KEYWORDS: *Biodegradable enantiomeric polylactides, Stereocomplex crystallites, Chain mobility*

INTRODUCTION

Development of biobased polymers to replace conventional petroleum-based polymers has received considerable attention with the growing awareness of sustainability. Polylactides (PLA), an environment friendly polymer from renewable resources, has received great attention in recent years.[1] Formation of stereocomplex (sc) crystallites between enantiomeric poly(L-lactide) (PLLA) and poly(D-lactide) (PDLA) has drawn much attention owing to much better physical properties than those of the constituting components since its first discovery by Ikada et al.[2] One of the most remarkable features of sc crystallites is its high melting point, 50 °C higher than that of PLLA or PDLA homochiral (hc) crystallites.[2−4] Sc crystallization has been proven to be one of the most effective methods to enhance the properties, including mechanical performance,[5−8] thermal stability,[9,10] and hydrolysis resistance,[11,12] of PLA. A 50:50 weight ratio between PLLA and PDLA generally promotes complete sc formation, but many factors including processing method,[9,13−18] processing conditions,[19−30] and molecular weight (M_w) of homopolymers have a profound influence on the relative amount of sc and hc crystallites. The physicochemical properties of PLA stereocomplexes strongly rely on the level of sc crystallinity. Thus, enhancing sc crystallization becomes a matter of concern.[9,21,23,29]

Sc crystallites are generally produced in a PLLA/PDLA blend with a 50:50 weight ratio from melt or solution.[4,31,32] Generally, the formation of hc crystallites of either PLLA or PDLA prevails over the formation of sc crystallites when the blends are prepared from high M_w PLLA and PDLA. The critical viscosity-average molecular weight is lower in the stereocomplexation from melt ($\bar{M}_v = 6 \times 10^3$ g mol^{-1}) than that from solution casting ($\bar{M}_v = 4 \times 10^4$ g mol^{-1}).[15,33,34] On the other hand, sc crystallites of high M_w PLA shows poor memory effect to reform sc after complete melting.[35] When pure sc crystallites are melted and crystallized again, hc crystallization always

Received: April 29, 2014
Revised: August 17, 2014
Published: August 18, 2014

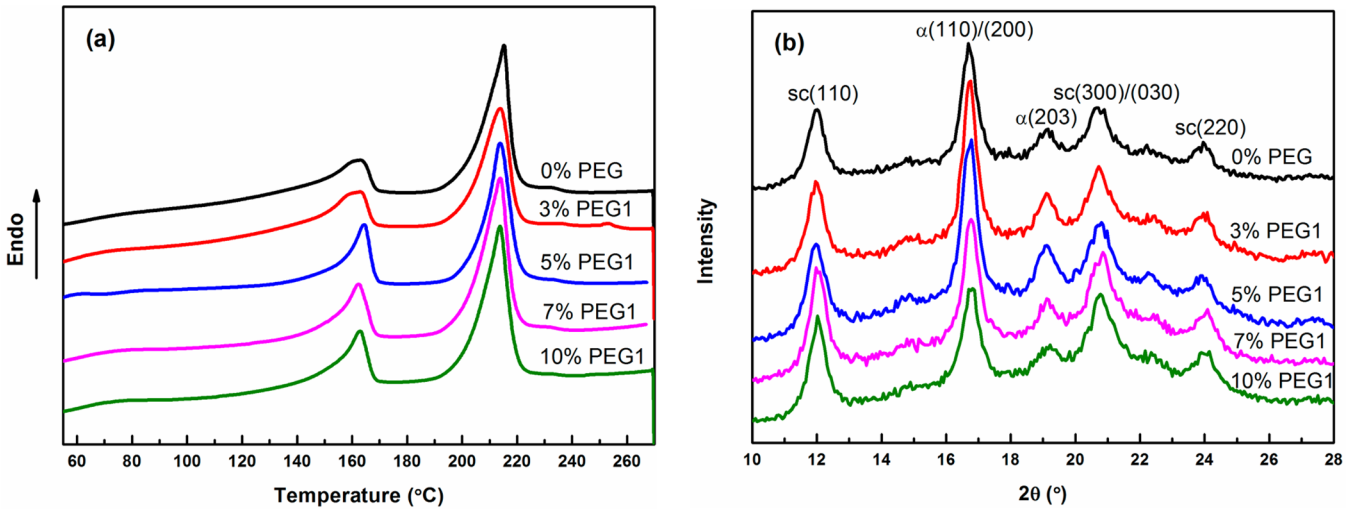

Figure 1. DSC heating curves (a) and WAXD profiles (b) of solution-blended PLLA/PDLA blends with different contents of PEG1.

prevails over the sc crystallization, leading to a coexistence of hc crystallites and sc crystallites. However, melt processing of polymers is much preferable in industry, so the efficient formation of sc crystallites from melt is extremely important due to the vast need of melt processing for various applications. Unfortunately, for high M_w PLA, exclusive formation of sc crystallites has never been achieved from the melt of a PLLA/PDLA blend.

Many studies are trying to achieve excellent efficiency in the formation of sc crystallites from melt, and several kinds of PLAs with different architectures have been applied.[18,35,36] Biela et al.[35] reported that the sc crystallites of star-shaped high M_w PLA with six arms or more can be formed perfectly after complete melting by minimizing the chain freedom due to hard lock-type interactions. Biela et al.[36] also presented the preparation method of linear high M_w sc crystallites after melting in the presence of PLA-functionalized multiwalled carbon nanotubes (MWCNT-*g*-PLA). Purnama et al.[18] proposed a new concept to enhance the formation of sc crystallites from melt by combining PLLA homopolymer and poly(D-lactide-*co*-ε-caprolactone) (PDLCL) random copolymer with a small content of ε-caprolactone (CL). The chain mobility and the reduced length of PDLA fragment caused by addition of CL fragment are the two driving forces to enhance the formation of sc crystallites from melt. The PDLA fragment in PDLCL has a shorter length compared to the PDLA homopolymer due to the presence of CL fragments. Then the effect of chain mobility of PLA on the formation of sc crystallites cannot be judged separately. Nevertheless, generally, complex processes are required to synthesize these polymers with special architectures, which significantly limits their utility in industrial applications, so it is more desirable if exclusive formation of sc crystallites can be achieved from the melt of commercial available, linear, high M_w PLLA/PDLA.

It is well known that PLLA chains have a relatively semirigid molecular backbone and poor chain mobility, which results in a very low crystallization rate.[37,38] Plasticization is effective to enhance the crystallization of PLLA, and the effect of plasticization on the crystallization behavior of PLLA has been studied widely.[1,39−43] Poly(ethylene glycol) (PEG) is the most investigated plasticizer for PLA. Plasticizer properties, including M_w, polarity, and end group, have been manipulated to increase the efficiency of plasticization.[1,39−41]

The crystallization rate of sc crystallites is much faster than that of hc crystallites.[25] Tsuji et al.[25] investigated the spherulite growth of sc crystallites in the blend of low M_w PLLA and PDLA from melt and the growth rate of hc crystallites in pure PLLA and PDLA films. Their work elucidated the mechanisms for rapid completion of overall sc crystallization compared with prolonged completion of overall hc crystallization of pure PLLA and PDLA.

However, the effect of chain mobility on the melt crystallization behavior of a PLLA/PDLA blend is still not clear, and no research has concentrated on the effect of plasticization on the crystallization behavior of a PLLA/PDLA blend until now. Herein, the effect of PEG on the melt crystallization behavior of high M_w PLLA/PDLA is studied. The points we are trying to address are as follows: (1) Is there any possibility for high M_w PLLA/PDLA melt to form sc crystallites exclusively to enlarge application? (2) For a PLLA/PDLA blend, does the low segmental mobility of PLA chains result in the limited formation of sc crystallites from high M_w PLA and by melt blending?

EXPERIMENTAL SECTION

Materials. A commercial PLLA (trade name 4032D, NatureWorks) was used. The M_w was 2.1 × 10^5 g mol^{-1}, and the polydispersity (PDI) was 1.7. The PDLA, synthesized by the ring-opening polymerization of D-lactic acid, was kindly supplied by Professor Chen Xue-Si at State Key Lab oratory of Polymer Physics and Chemistry, China. The M_w of PDLA was about 1.0 × 10^5 g mol^{-1}, and the PDI of PDLA was 1.7. PEGs with M_w of 1000 g mol^{-1} (PEG1), 2000 g mol^{-1} (PEG2), 4000 g mol^{-1} (PEG4), and 6000 g mol^{-1} (PEG6) were purchased from Aladdin Industrial Inc.

Sample Preparation. The blends were prepared by solution blending. Briefly, the separately prepared solutions of PLLA, PDLA, and PEG using dichloromethane as the solvent were mixed vigorously. Then, the blends were obtained by solvent evaporation at room temperature and further vacuum-drying to remove residual solvent. The content of PEG was ranged from 0 to 10 wt % based on the total weight of the PLLA/PDLA/PEG blends, with the weight ratio of PLLA to PDLA maintained at 1:1. Taking PEG content of 10 wt % as an example, the weight ratio of the components is PLLA:PDLA:PEG =45:45:10 wt %.

Characterizations. The thermal properties of the blends were characterized by differential scanning calorimetry (DSC) with a DSC Q20 (TA Instruments, U.S.A.) under a 50 mL min^{-1} nitrogen gas flow. The blends from solution blending and subsequent strict drying were

heated at a rate of 10 °C/min. Melt crystallization was evaluated from a deeply equilibrated melt state (270 °C) according to ref 44. The blends were melted at 270 °C for 2 min to erase previous thermal history, and then the melt was cooled to 0 °C and heated again. The heating and cooling rates were set to be 10 °C/min. For the evaluation of the glass transition temperature (T_g), the samples were quenched to 0 °C after melting at 270 °C for 2 min and then heated to 270 °C at a rate of 10 °C/min.

The crystalline structures of the blends were characterized using wide-angle X-ray diffraction (WAXD). WAXD profiles were recorded on a DX-1000 X-ray diffractometer (Dandong Fanyuan Instrument Co., Ltd.) using a Cu Kα radiation source (λ = 0.154056 nm, 40 kV, 25 mA) in the scanning angle range of 2θ = 5−50° at a scanning speed of 3°/min. The crystallinity of the hc crystallites (X_c(hc)), sc crystallites (X_c(sc)), and both crystallites (X_c(hc+sc)) were determined from WAXD profiles according to Tsuji et al.[13,14] The fraction of sc crystallites, f_{sc}, can be obtained from the following equation

$$f_{sc} = \frac{X_c(sc)}{X_c(hc) + X_c(sc)}$$

The spherulite growth of sc crystallites during the isothermal crystallization process was observed using an Olympus BX51 polarizing optical microscopy (POM, Olympus Co., Tokyo, Japan) equipped with MicroPublisher 5.0 RTV CCD and Linkam FTIR600 heating and cooling stage under nitrogen gas protection. The samples were first melted at 270 °C for 2 min to remove the thermal history. Then, they were cooled at 50 °C/min to the crystallization temperature (T_c) of 170 °C for isothermal crystallization.

RESULTS AND DISCUSSION

Effect of PEG Content on Formation of sc Crystallites.

DSC heating curves and WAXD profiles of solution-blended PLLA/PDLA blends with different contents of PEG1 are shown in Figure 1. As shown in Figure 1a, two main endothermic peaks are observed in the vicinity of 165 and 215 °C for all PLLA/PDLA/PEG1 blends, indicating the melting of hc and sc crystallites, respectively. In Figure 1b, the diffraction peaks of hc crystallites at 2θ values of 16.7° and 18.4°, corresponding to the (200) and/or (110) planes and the (203) plane of the α or δ form crystals of PLLA or PDLA,[45] and diffraction peaks of sc crystallites at 2θ values of 11.6°, 20.6°, and 23.5°, corresponding to the (110) plane, (300) and/or (030) planes, and (220) plane,[31] can be observed. Both DSC and WAXD results indicate that the formation of sc crystallites is accompanied by the formation of hc crystallites due to the high M_w PLLA and PDLA were used, although the samples were prepared by solution blending.

DSC cooling curves of PLLA/PDLA blends with different contents of PEG1 from a deeply equilibrated melt state (270 °C) are shown in Figure 2, and the crystallization parameters are collected in Table 1. The zero population of racemic helical pairs is reported to be at about 260 °C, consistent with the value of the equilibrium melting temperature of sc crystallites (Tm° = 259 ± 3 °C) determined via a combination of small-angle X-ray scattering (SAXS), WAXD, and DSC results.[44] As shown in Figure 2, no exothermal peak can be observed for the neat PLLA/PDLA blend. The presence of PEG enhances the crystallizability greatly, and pronounced crystallization peaks are recorded for PLLA/PDLA/PEG blends. Moreover, with the increase in PEG1 content, the crystallization temperature (T_c) increases continuously, and the crystallization enthalpy (ΔH_c) increases significantly.

DSC heating curves and WAXD profiles of the samples obtained in Figure 2 are shown in Figure 3, and the cold

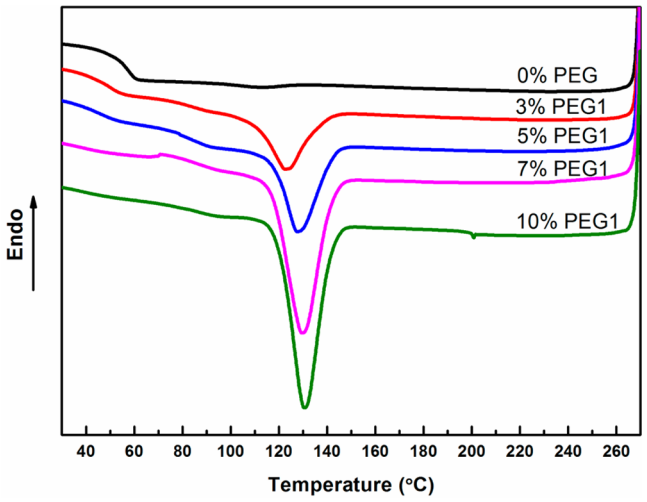

Figure 2. DSC cooling curves of PLLA/PDLA blends with different contents of PEG1 after melting at 270 °C.

Table 1. DSC Data of PLLA/PDLA Blends with Different Contents of PEG1 during Melt Crystallization

PLLA/PDLA/PEG	T_c (°C)	ΔH_c (J/g)	T_{cc} (°C)	ΔH_{cc} (J/g)
0% PEG			114.0	32.6
3% PEG1	122.5	20.4	103.4	12.3
5% PEG1	127.4	30.0	101.8	7.4
7% PEG1	129.4	38.6	95.5	1.5
10% PEG1	130.7	39.8		

crystallization parameters are also included in Table 1. From Figure 3a, for the neat PLLA/PDLA blend, two main melting peaks at around 165 and 210 °C are observed, indicating the melting of hc and sc crystallites, respectively. The double melting behavior of hc crystallites can be attributed to the effect of crystallization temperature on the crystalline structures of hc crystallites.[46−48] The appearance of the noticeable cold crystallization peak at 114.0 °C reflects the fact that the blend contains crystallizable free amorphous region. The cold crystallization behavior depends on the content of PEG1. With the increase in PEG1 content, both cold crystallization temperature (T_{cc}) and cold crystallization enthalpy (ΔH_{cc}) decrease due to increased crystallizability. For the blend with 10 wt % PEG1, the cold crystallization peak disappears, indicating that crystallization can be completed during the previous cooling process. Moreover, the melting behavior depends on the PEG1 content as well. As shown in Figure 3a, the melting peak intensity of hc crystallites decreases and that of the sc crystallites increases with increasing PEG1 content. When the PEG1 content increases to 10 wt %, the melting peak of the hc crystallites disappears, and a single melting peak of sc crystallites can be observed. The dependence of the melting behavior on PEG1 content demonstrates that the formation of hc and sc crystallites depends on the PEG1 content. As shown in Figure 3b, no diffraction peaks can be observed for the neat PLLA/PDLA blend due to the poor crystallizability during the cooling process shown in Figure 2, indicating that neither hc nor sc crystallites can be formed during the cooling process in the neat PLLA/PDLA blend. With the increase in PEG1 content, the diffraction intensity of sc crystallites enhances and that of hc crystallites becomes weak. When PEG1 content increases to 10 wt %, the diffraction peaks of hc crystallites disappear, and only the diffraction peaks of sc crystallites can be

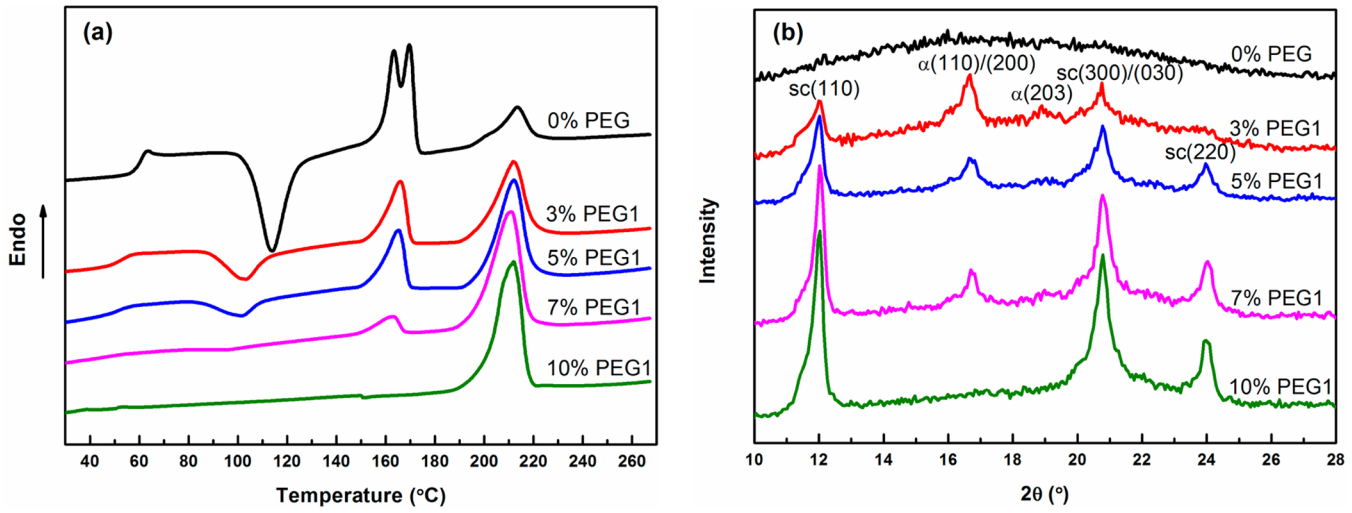

Figure 3. DSC heating curves (a) and WAXD profiles (b) of the samples obtained in Figure 2.

observed, indicating that exclusive sc crystallites are achieved. This is in marked contrast with the results for the solution blended sample, where the formation of sc crystallites is always accompanied by hc crystallites.

The crystallinity and fraction of sc crystallites by the WAXD method for the PLLA/PDLA blends with different PEG1 content are given in Figure 4. The unfilled square represents

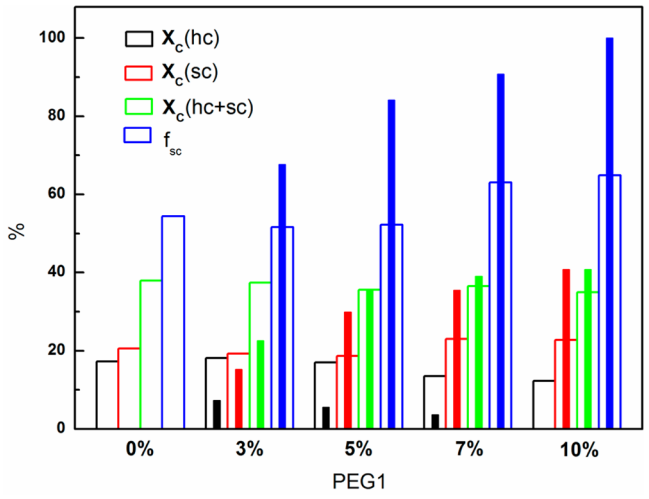

Figure 4. Crystallinity and the fraction of sc crystallites by WAXD method for PLLA/PDLA blends with different contents of PEG1. The unfilled square represents the solution blended samples, and the filled square represents the samples experienced melt crystallization.

the solution blended samples, and the filled square represents the samples that experienced melt crystallization. It should be noted that compared to the melt crystallized sample the addition of different contents of PEG1 has less effect on the formation of sc crystallites in the case of solution blending. For blends with 3 and 5 wt % PEG1, X_c(hc), X_c(sc), X_c(hc+sc), and f_{sc} change little compared to those of the neat PLLA/PDLA blend. When PEG1 content increases to 7 and 10 wt %, f_{sc} increases by about 10%. After melt crystallization, for the neat PLLA/PDLA blend, X_c(hc), X_c(sc), X_c(hc+sc), and f_{sc} are 0%. With the addition of 3 wt % PEG1, X_c(hc+sc) is improved dramatically to be above 20%, and due to the crystallizability of PLLA/PDLA, it is enhanced greatly by the plasticizing effect of PEG. X_c(hc+sc) increases with increasing PEG1 content, and it is at the same level for the blend with 7 and 10 wt % of PEG1. Moreover, with increasing PEG1 content, X_c(hc) decreases, and it reduces to 0% for the blend with 10 wt % PEG1. X_c(sc) and f_{sc} increase as the content of PEG1 increases, and 100% of f_{sc} is achieved for the blend with 10 wt % PEG1. Overall, for the blends with different PEG1 content, f_{sc} of the samples after melt crystallization is higher than that of the blends prepared by solution casting. For the blends with PEG1 above 5 wt %, X_c(sc) is even higher than that of the blends by solution casting. These results clearly show that the addition of PEG in the PLLA/PDLA blends can enhance the formation of sc crystallites from the melt, and exclusive sc crystallites can be achieved from the PLLA/PDLA melt with the addition of 10 wt % PEG1.

Effect of M_w of PEG on Formation of sc Crystallites. DSC heating curves and WAXD profiles of the solution-blended PLLA/PDLA blends with 10 wt % PEG of different M_w are shown in Figure 5. The melting peaks at around 165 and 215 °C in the DSC curves and the diffraction peaks of hc and sc crystallites presented on WAXD profiles for the solution-casted blend clearly indicate the formation of both hc and sc crystallites, respectively.

DSC cooling curves of the PLLA/PDLA blends with 10 wt % PEG of different M_w after melting at 270 °C are shown in Figure 6, and the crystallization parameters are collected in Table 2. As shown in Figure 6, the improvement of crystallizability depends on the M_w of PEG. With an increase in M_w of PEG, T_c and ΔH_c decrease. For the blends with PEG4, the crystallization peak splits into two peaks with a shoulder at the low temperature. The peak temperature of the shoulder shifts to even lower temperature for the blends with PEG6, while the peak temperature of main peak is less affected, almost the same as that of the blend with PEG2. The shoulder peak at lower temperature may be associated with hc crystallization, and the main peak at higher temperature is related to sc crystallization.

DSC heating curves and WAXD profiles of the samples obtained in Figure 6 are shown in Figure 7, and the cold crystallization parameters are also shown in Table 2. The formation of hc and sc crystallites depends on the addition of PEG and the M_w of PEG. For the blends with PEG1 and PEG2, the DSC melting curves show a single peak at around 215 °C in

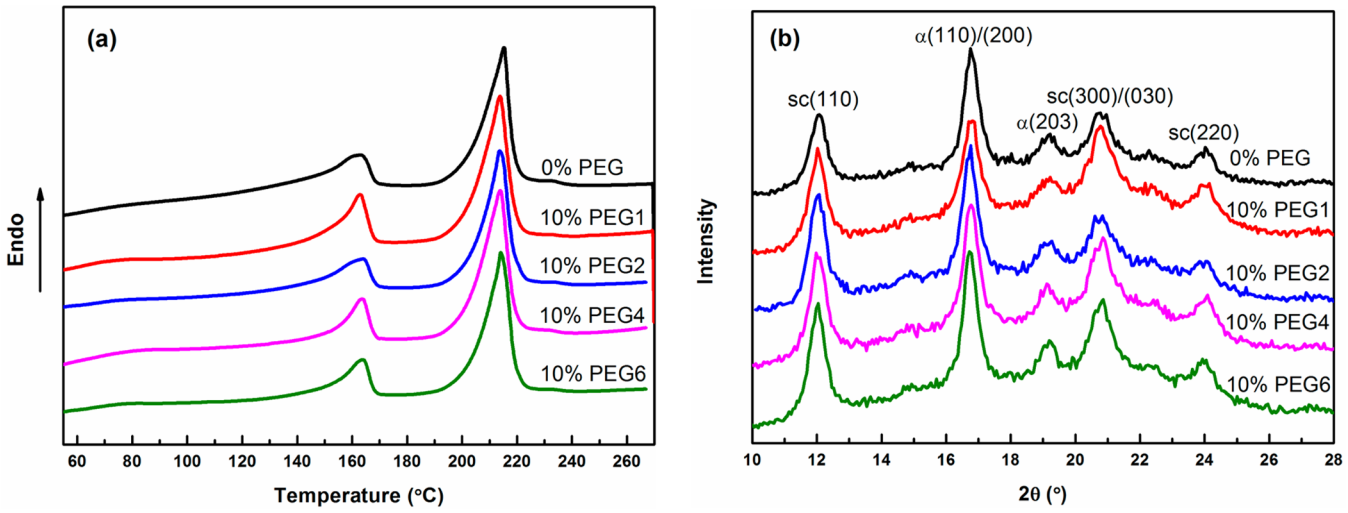

Figure 5. DSC heating curves (a) and WAXD profiles (b) of solution blended PLLA/PDLA blends with 10 wt % PEG of different M_w.

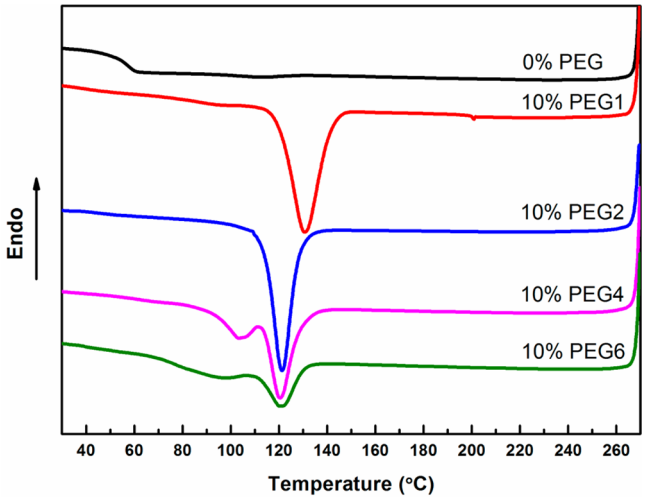

Figure 6. DSC cooling curves of PLLA/PDLA blends with 10 wt % PEG of different M_w after melting at 270 °C.

Table 2. DSC Data of PLLA/PDLA Blends with 10 wt % PEG of Different M_w during Melt Crystallization

PLLA/PDLA/PEG	T_c (°C)	ΔH_c (J/g)	T_{cc} (°C)	ΔH_{cc} (J/g)
0% PEG			114.0	32.6
10% PEG1	130.7	39.8		
10% PEG2	121.2	36.2		
10% PEG4	104.5, 120.8	33.4		
10% PEG6	95.7, 120.4	24.4	93.9	2.5

Figure 7a, showing the formation of complete sc crystallites without hc crystallites. Strong diffraction peaks of sc crystallites and no diffraction peaks of hc crystallites presented on the WAXD profile in Figure 7b also indicate that sc crystallites are the exclusive crystalline species and no hc crystallites form. However, the blends with PEG4 and PEG6 show two melting peaks at about 165 and 215 °C in Figure 7a, indicating the formation of both hc and sc crystallites. Moreover, a weak cold crystallization peak with T_{cc} of 93.9 °C presents for the blend with PEG6 due to the extent of improvement of crystallizability decreasing with increasing M_w of PEG as shown in Figure 6. Consistent with the DSC results, in addition to the diffraction peaks of sc crystallites at 2θ values of 11.6°, 20.6°, and 23.5°, diffraction peaks of hc crystallites appear on the WAXD profiles for the blends with PEG4 and PEG6 in Figure 7b.

The crystallinity and fraction of sc crystallites by the WAXD method for the PLLA/PDLA blends with 10 wt % PEG of different M_w are given in Figure 8. The unfilled square represents the solution blended samples, and the filled square represents the samples that experienced melt crystallization. After melt crystallization, for the neat PLLA/PDLA blend, X_c(hc), X_c(sc), X_c(hc+sc), and f_{sc} are 0%. With the addition of PEG, X_c(hc+sc) improves dramatically to be above 30% due to the crystallizability of the PLLA/PDLA blends being enhanced greatly by the plasticizing effect of PEG. Moreover, the formation of hc and sc crystallites depends on the M_w of PEG. With an increase in M_w of PEG, X_c(hc) increases, X_c(sc) reduces, and f_{sc} decreases gradually. f_{sc} values are 100% for the blends with PEG1 and PEG2, indicating exclusive sc crystallites can be achieved in the blends with PEG1 and PEG2. X_c(sc) values reach 40.8% and 32.8% for the blends with PEG1 and PEG2, respectively. f_{sc} decreases to 65% for the blend with PEG4, and it holds a value of 37.2% for the blend with PEG6.

For the solution blended samples, with increasing M_w of PEG, X_c(hc), X_c(sc), X_c(hc+sc), and f_{sc} almost keep constant. Moreover, with the addition of PEG, X_c(hc) reduces to be about 13%, which is 17% for the neat PLLA/PDLA blend. X_c(sc) increases by about 2%, and f_{sc} increases by about 10%. The results demonstrate that the presence of PEG of different M_w also has less effect on the formation of sc crystallites in the case of solution blending compared with that of the samples that experienced melt crystallization. Compared with the blends prepared by solution casting in which sc crystallization is always accompanied by hc crystallization, exclusive sc crystallites are achieved in the blends with PEG1 and PEG2 after melt crystallization. Even for the blend with PEG4, both X_c(sc) and f_{sc} after melt crystallization approach that of solution casting. However, neither hc nor sc crystallites can be formed during the cooling process in the neat PLLA/PDLA blend. These results show that addition of PEG in the PLLA/PDLA blends can enhance the formation of sc crystallites from the melt, and exclusive sc crystallites can be formed from the melt with the addition of 10 wt % PEG1 or PEG2.

Mechanism of Enhanced Formation of sc Crystallites of High M_w PLLA/PDLA from Melt. For the melt crystallized samples, the crystallizability of the PLLA/PDLA blends can be

dx.doi.org/10.1021/sc500464c | ACS Sustainable Chem. Eng. 2014, 2, 2301−2309

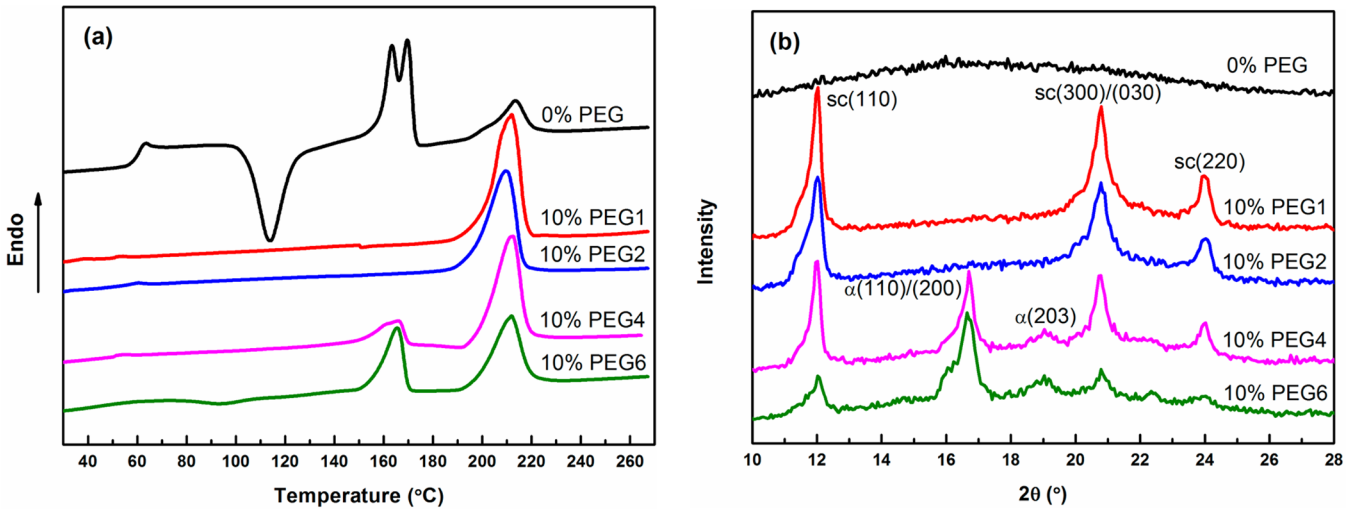

Figure 7. DSC heating curves (a) and WAXD profiles (b) of samples obtained in Figure 6.

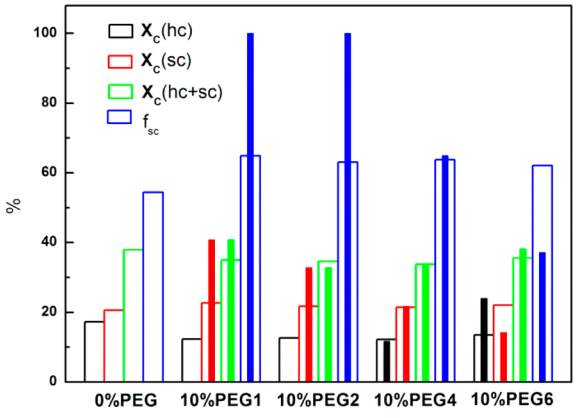

Figure 8. Crystallinity and the fraction of sc crystallites by WAXD method for neat PLLA/PDLA blend and PLLA/PDLA blends with 10 wt % PEG of different M_w. The unfilled square represents the solution blended samples, and the filled square represents the samples experienced melt crystallization.

enhanced greatly by the presence of PEG. For the neat PLLA/PDLA blend, no exothermal peak can be observed on the DSC cooling curve, and no diffraction peaks can be observed on the corresponding WAXD profile due to poor crystallizability during the cooling process. Then X_c(hc), X_c(sc), X_c(hc+sc), and f_{sc} are 0%. These results indicate that for the neat PLLA/PDLA blend both the crystallization of hc and sc crystallites hardly occur under the cooling rate of 10 °C/min. On the one hand, even it is reported that the crystallization rate of sc crystallites is much faster than that of hc crystallites,[13] the crystallization of sc crystallites hardly occurs under the cooling rate of 10 °C/min. On the other hand, even sc crystallites have been evidenced to be an efficient and biodegradable nucleating agent for hc crystallization;[49] the crystallization of hc crystallites cannot occur due to the lack of sc crystallites. The introduction of PEG increases the ability of the PLLA/PDLA blends to crystallize. The improvement depends on the M_w and the content of PEG. The crystallization peak is significantly sharpened, which is enhanced by higher PEG content and also by lower M_w of PEG, and this pushed the T_c closer to the onset crystallization temperature. Accordingly, the enhanced crystallizability of the PLLA/PDLA blends is also manifested by a decrease in T_{cc} and ΔH_{cc} during the heating process. When the content of PEG1 increases to 10 wt %, no cold crystallization takes place during the heating process after melting (Figure 3a). When the M_w of PEG increases to 6000 g mol^{-1}, cold crystallization occurs during the heating process for the blend with 10 wt % PEG (Figure 7a). The enhanced crystallizability of the PLLA/PDLA blends by the presence of PEG can be attributed to the increased segmental mobility of the PLA chains. The miscibility of the PLLA/PEG blends depends on the molecular weight of PEG and/or blend compositions.[40] It is reported that PEG (M_w = 3.5 × 10^3 g mol^{-1}) or poly(ethylene oxide) (PEO; M_w = 1.5 × 10^5 g mol^{-1}) are both miscible with PLA in the blends below a content of 20 wt %.[50] Table 3 shows the glass transition temperature (T_g) of the PLLA/PDLA/PEG blends. The results show clearly a decrease in T_g due to enhanced segmental mobility of PLA chains caused by the presence of PEG, and T_g decreases with an increase in content of PEG or a decrease in PEG M_w. The lower M_w of the plasticizer enables increased miscibility with PLA and more efficient reduction of T_g.[41]

The crystalline structures of the melt-crystallized samples depend on the M_w and the content of PEG. X_c(sc) of the blends increases with increasing content or decreasing M_w of PEG as shown in Figures 4 and 8. The dependence of crystalline structures on the M_w and the content of PEG demonstrates that the segmental mobility of PLA chains plays a dominant role on the formation of sc crystallites. With an increase in content of PEG1 or a decrease in the M_w of PEG, T_g decreases and X_c(sc) increases. Exclusive sc crystallites can be achieved in the blends with 10 wt % PEG1 and PEG2, and no

Table 3. Glass Transition Temperature (T_g) of PLLA/PDLA/PEG Blends

			PEG1				10%	
PLLA/PDLA/PEG	0%	3%	5%	7%	10%	PEG2	PEG4	PEG6
T_g (°C)	61.9	53.4	52.9	49.4	36.9	46.9	52.0	52.3

dx.doi.org/10.1021/sc500464c | ACS Sustainable Chem. Eng. 2014, 2, 2301−2309

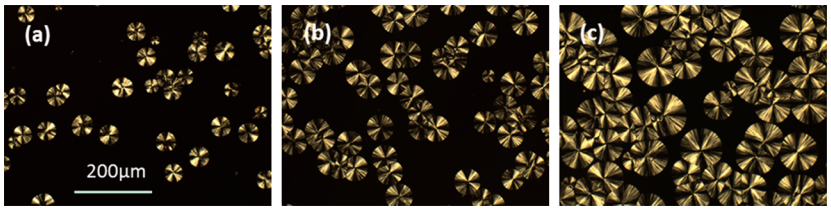

Figure 9. POM micrographs of PLLA/PDLA blends with 0 wt % (a), 3 wt % (b), and 10 wt % (c) PEG1 isothermally crystallized at 170 °C for 10 min. The scale bar in (a) represents 200 μm and is applied to all other micrographs.

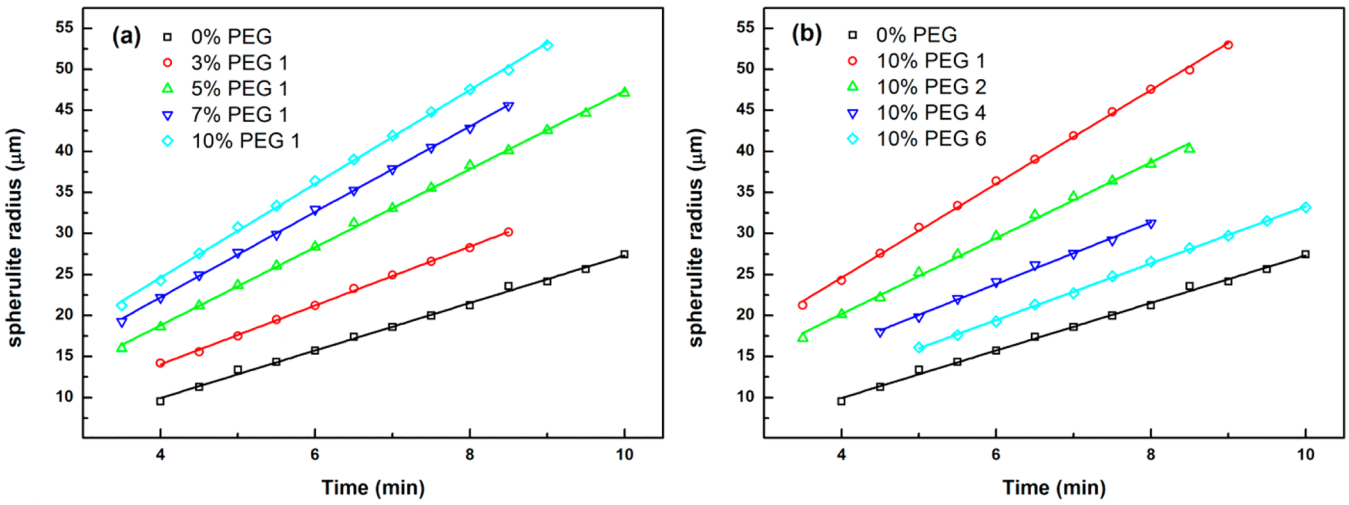

Figure 10. Changes of spherulite radius as functions of crystallization time for PLLA/PDLA blends with different contents of PEG1 (a) and 10% PEG of different M_w (b) during isothermal crystallization at 170 °C.

crystallizable free amorphous region can be observed as shown in Figure 7. Plasticizer increases the segmental mobility of the polymer chains and enhances the crystallization rate by reducing the energy required during crystallization for the chain folding process. Tsuji et al.[28] investigated the crystallization behavior of high molecular weight PLLA and PDLA blended at different ratios. The results shown that solely hc crystallites mixtures of PLLA and PDLA were synchronously and separately formed during isothermal crystallization in the temperature range of 90−130 °C, irrespective of the blending ratio, whereas in addition to hc crystallites, sc crystallites were formed in the blends with a weight ratio of 50:50 at T_c above 150 and 160 °C. The crystallization rate of sc crystallites is much faster than that of hc crystallites,[25] and further enhancement of the crystallization rate of sc crystallites by PEG reduces the amount of residual homopolymer for hc crystallization. More importantly, the chain mobility helps PDLA to confront with PLLA and enhances the interaction between PLLA and PDLA macromolecules. The crystallization of sc crystallites requires racemic helical pairs of PLLA and PDLA to reach the growth front. This requirement sets a very stringent limitation to the growth of the sc crystallites from high M_w PLA during melt blending due to a relatively semirigid molecular backbone of PLA chains in that there may be local enrichment (or depletion) of the PLA species that is needed, and sc crystallization is limited by the local nonavailability of the enantiomer that would allow further growth. As the M_w of PEG increases or the content of PEG decreases, the segmental mobility of PLA chains is not enough for complete formation of sc crystallites in the limited time caused by the cooling rate of 10 °C/min, and then, the epitaxial growth of hc on sc crystallites occurs. The formation of a large number of hc crystallites splits the crystallization peak into two peaks with a shoulder at low temperature.

To quantitatively demonstrate the effect of PEG on the spherulitic growth rates of sc crystallites, isothermal crystallization is performed at 170 °C, a temperature above the melting temperature of hc crystallites, and only the crystallization of sc crystallites can occur. Figure 9 shows the POM micrographs of the PLLA/PDLA blends with 0, 3, and 10 wt % PEG1 isothermally crystallized at 170 °C for 10 min. Spherulites are the common morphology of sc crystallization for the neat PLLA/PDLA blend and PLLA/PDLA blends with PEG. The size of spherulites for the neat PLLA/PDLA blend is relatively small after crystallization for 10 min, and the size of spherulites for the PLLA/PDLA blend with 10 wt % PEG1 is apparently larger than that with 3 wt % PEG1, indicating that PEG can accelerate the spherulitic growth rates of sc crystallites. Figure 10 shows the changes of spherulite radius as functions of crystallization time for the PLLA/PDLA blends with different content of PEG1 and 10 wt % PEG of different M_w during isothermal crystallization at 170 °C. With the content of PEG1 increasing, the spherulitic growth rate of sc crystallites increases. The spherulitic growth rates of sc crystallites (slopes of the linear fitted lines in Figure 10) for the PLLA/PDLA blends with 0, 3, 5, 7, 10 wt % PEG1 at 170 °C are evaluated to be 2.9, 3.6, 4.8, 5.2, and 5.7 μm/min, respectively. It should be noticed that the spherulitic growth rate of the PLLA/PDLA blend with 10% PEG1 is almost twice as that of the neat PLLA/PDLA blend even at T_c as high as 170 °C. The increased spherulitic growth rate of the sc crystallites can be observed for the PLLA/PDLA blends with 10% PEG of different M_w as well. As shown in Figure 10b, with the M_w of PEG increasing, the acceleration of the spherulitic growth rate

of sc crystallites weakens. The spherulitic growth rate of sc crystallites for the neat PLLA/PDLA blend and PLLA/PDLA blends with 10% PEG1, PEG2, PEG4, PEG6 are evaluated to be 2.9, 5.7, 4.6, 3.8, and 3.5 μm/min, respectively.

It should be noted that compared with the samples that experienced melt crystallization, the addition of PEG has less effect on the formation of sc crystallites in the case of solution blending. In the case of solution blending, for blends with 10 wt % PEG of different M_w, f_{sc} increased by about 10% compared with that of the neat PLLA/PDLA blend (Figure 8). For the blends with 3 and 5 wt % PEG1, X_c(hc), X_c(sc), X_c(hc+sc), and f_{sc} change little compared to those of the neat PLLA/PDLA blend. When the content of PEG1 increases to 7 and 10 wt %, f_{sc} increases by about 10% (Figure 4). These results may be caused by the solution being dilute, where the chain mobility of the polymer is high and the solvent helps the polymer segments to diffuse to the growth front of sc crystallites. Complete sc crystallites could not be obtained even by solution blending as shown in Figures 1 and 5. The reason is that the rate of racemic crystallization is quite low compared to that of the solvent evaporation if PLA has a M_w higher than 1×10^5 g mol^{-1}, although racemic crystallization proceeds more quickly than homopolymer crystallization in microscopically well-mixed solutions.[51]

As summarized in Figures 4 and 8, the introduction of PEG in the PLLA/PDLA blends enhances the melt crystallization of sc crystallites. Furthermore, compared with the blends prepared by solution casting, in which sc crystallization is always accompanied by hc crystallization, exclusive sc crystallites can be achieved in the blends with 10 wt % PEG1 and PEG2 after melt crystallization, and no crystallizable free amorphous region can be observed as shown in Figure 6. This means that exclusive sc crystallites with no crystallizable free amorphous region can be achieved in high M_w PLLA and PDLA by melt processing in the presence of PEG. It suggests that low chain mobility may be the main reason for the limitation of sc crystallites formation from high M_w PLA and by melt processing.

CONCLUSION

We found an easy but effective way to enhance the melt crystallization of sc crystallites from high M_w PLA by the addition of PEG. The presence of PEG has less effect on the formation of sc crystallites during solution blending compared with the melt crystallized samples, and the formation of sc crysltallites is always accompanied by hc crystallites during solution blending. However, the crystallizability of the PLLA/PDLA blend can be enhanced greatly by the addition of PEG during the crystallization from the melt, and the effect is enhanced by higher content and lower M_w of PEG. The crystalline structures depend on the M_w and the content of PEG, and X_c(sc) increases with decreased M_w or increased content of PEG. The dependence of crystalline structures on the M_w and the content of PEG demonstrates that segmental mobility of PLAs chains plays a dominant role on the formation of sc crystallites. POM observation shows that the spherulitic growth rate of sc crystallites can be accelerated by PEG. The results suggest that the low chain mobility may be the main reason for the limited formation of sc crystallites from high M_w PLA and by melt processing.

AUTHOR INFORMATION

Corresponding Author

*Tel.: + 86 28 8546 0130. Fax: + 86 28 8546 0130. E-mail: weiyang@scu.edu.cn.

Notes

The authors declare no competing financial interest.

ACKNOWLEDGMENTS

This work was supported by the National Natural Science Foundation of China (NNSFC Grants 21374065 and 51033003), Major State Basic Research Development Program of China (973 program) (Grant No. 2011CB606006 and 2012CB025902), and the Innovation Team Program of Science & Technology Department of Sichuan Province (Grant 2013TD0013). We also thanks Prof. Chaobin He from the National University of Singapore for extremely helpful suggestions on our work.

REFERENCES

(1) Saeidlou, S.; Huneault, M. A.; Li, H.; Park, C. B. Poly(lactic acid) crystallization. *Prog. Polym. Sci.* **2012**, *37* (12), 1657−1677.

(2) Ikada, Y.; Jamshidi, K.; Tsuji, H.; Hyon, S. H. Stereocomplex formation between enantiomeric poly(lactides). *Macromolecules* **1987**, *20* (4), 904−906.

(3) Pan, P.; Inoue, Y. Polymorphism and isomorphism in biodegradable polyesters. *Prog. Polym. Sci.* **2009**, *34* (7), 605−640.

(4) Tsuji, H. Poly(lactide) stereocomplexes: Formation, structure, properties, degradation, and applications. *Macromol. Biosci.* **2005**, *5* (7), 569−597.

(5) Tsuji, H.; Ikada, Y. Stereocomplex formation between enantiomeric poly(lactic acid)s. XI. Mechanical properties and morphology of solution-cast films. *Polymer* **1999**, *40* (24), 6699−6708.

(6) Zhang, X.; Nakagawa, R.; Chan, K. H. K.; Kotaki, M. Mechanical property enhancement of polylactide nanofibers through optimization of molecular weight, electrospinning conditions, and stereocomplexation. *Macromolecules* **2012**, *45* (13), 5494−5500.

(7) Sun, Y.; He, C. Synthesis and stereocomplex crystallization of poly(lactide)−graphene oxide nanocomposites. *ACS Macro Lett.* **2012**, 709−713.

(8) Sun, Y.; He, C. Synthesis, stereocomplex crystallization, morphology and mechanical property of poly(lactide)-carbon nanotube nanocomposites. *RSC Adv.* **2013**, *3* (7), 2219−2226.

(9) Purnama, P.; Kim, S. H. Stereocomplex formation of high-molecular-weight polylactide using supercritical fluid. *Macromolecules* **2010**, *43* (2), 1137−1142.

(10) Tsuji, H.; Fukui, I. Enhanced thermal stability of poly(lactide)s in the melt by enantiomeric polymer blending. *Polymer* **2003**, *44* (10), 2891−2896.

(11) Tsuji, H. In vitro hydrolysis of blends from enantiomeric poly(lactide)s. Part 1. Well-stereo-complexed blend and non-blended films. *Polymer* **2000**, *41* (10), 3621−3630.

(12) Tsuji, H. In vitro hydrolysis of blends from enantiomeric poly(lactide)s. Part 4: Well-homo-crystallized blend and nonblended films. *Biomaterials* **2003**, *24* (4), 537−547.

(13) Tsuji, H.; Yamamoto, S. Enhanced stereocomplex crystallization of biodegradable enantiomeric poly(lactic acid)s by repeated casting. *Macromol. Mater. Eng.* **2011**, *296* (7), 583−589.

(14) Tsuji, H.; Nakano, M.; Hashimoto, M.; Takashima, K.; Katsura, S.; Mizuno, A. Electrospinning of poly(lactic acid) stereocomplex nanofibers. *Biomacromolecules* **2006**, *7* (12), 3316−3320.

(15) Tsuji, H.; Ikada, Y. Stereocomplex formation between enantiomeric poly(lactic acids). 9. Stereocomplexation from the melt. *Macromolecules* **1993**, *26* (25), 6918−6926.

(16) Tsuji, H.; Hyon, S. H.; Ikada, Y. Stereocomplex formation between enantiomeric poly(lactic acid)s. 4. Differential scanning calorimetric studies on precipitates from mixed solutions of poly(D-

lactic acid) and poly(L-lactic acid). *Macromolecules* **1991**, *24* (20), 5657−5662.
(17) Purnama, P.; Hyun Kim, S. Rapid stereocomplex formation of polylactide using supercritical fluid technology. *Polym. Int.* **2012**, *61* (6), 939−942.
(18) Purnama, P.; Jung, Y.; Kim, S. H. Stereocomplexation of poly(L-lactide) and random copolymer poly(D-lactide-co-ε-caprolactone) to enhance melt stability. *Macromolecules* **2012**, *45* (9), 4012−4014.
(19) Sun, J.; Yu, H.; Zhuang, X.; Chen, X.; Jing, X. Crystallization behavior of asymmetric PLLA/PDLA blends. *J. Phys. Chem. B* **2011**, *115* (12), 2864−2869.
(20) Sun, J. R.; Shao, J.; Huang, S. Y.; Zhang, B.; Li, G.; Wang, X. H.; Chen, X. S. Thermostimulated crystallization of polylactide stereocomplex. *Mater. Lett.* **2012**, *89*, 169−171.
(21) Bao, R.-Y.; Yang, W.; Jiang, W.-R.; Liu, Z.-Y.; Xie, B.-H.; Yang, M.-B.; Fu, Q. Stereocomplex formation of high-molecular-weight polylactide: A low temperature approach. *Polymer* **2012**, *53* (24), 5449−5454.
(22) Bao, R.-Y.; Yang, W.; Jiang, W.-R.; Liu, Z.-Y.; Xie, B.-H.; Yang, M.-B. Polymorphism of racemic poly(L-lactide)/poly(D-lactide) blend: Effect of melt and cold crystallization. *J. Phys. Chem. B* **2013**, *117* (13), 3667−3674.
(23) Fujita, M.; Sawayanagi, T.; Abe, H.; Tanaka, T.; Iwata, T.; Ito, K.; Fujisawa, T.; Maeda, M. Stereocomplex formation through reorganization of poly(L-lactic acid) and poly(D-lactic acid) Crystals. *Macromolecules* **2008**, *41* (8), 2852−2858.
(24) Zhang, J. M.; Tashiro, K.; Tsuji, H.; Domb, A. J. Investigation of phase transitional behavior of poly(L-lactide)/poly(D-lactide) blend used to prepare the highly-oriented stereocomplex. *Macromolecules* **2007**, *40* (4), 1049−1054.
(25) Tsuji, H.; Tezuka, Y. Stereocomplex formation between enantiomeric poly(lactic acid)s. 12. Spherulite growth of low-molecular-weight poly(lactic acid)s from the melt. *Biomacromolecules* **2004**, *5* (4), 1181−1186.
(26) Brochu, S.; Prud'homme, R. E.; Barakat, I.; Jerome, R. Stereocomplexation and morphology of polylactides. *Macromolecules* **1995**, *28* (15), 5230−5239.
(27) Maillard, D.; Prud'homme, R. E. Differences between crystals obtained in PLLA-rich or PDLA-rich stereocomplex mixtures. *Macromolecules* **2010**, *43* (9), 4006−4010.
(28) Tsuji, H.; Tashiro, K.; Bouapao, L.; Hanesaka, M. Synchronous and separate homo-crystallization of enantiomeric poly(L-lactic acid)/poly(D-lactic acid) blends. *Polymer* **2012**, *53* (3), 747−754.
(29) Na, B.; Zhu, J.; Lv, R.; Ju, Y.; Tian, R.; Chen, B. Stereocomplex formation in enantiomeric polylactides by melting recrystallization of homocrystals: Crystallization Kinetics and crystal morphology. *Macromolecules* **2014**, *47* (1), 347−352.
(30) Zhu, J.; Na, B.; Lv, R. H.; Li, C. Enhanced stereocomplex formation of high-molecular-weight polylactides by gelation in an ionic liquid. *Polym. Int.* **2014**, *63* (6), 1101−1104.
(31) Cartier, L.; Okihara, T.; Lotz, B. Triangular polymer single crystals: Stereocomplexes, twins, and frustrated structures. *Macromolecules* **1997**, *30* (20), 6313−6322.
(32) Tan, B. H.; Hussain, H.; Leong, Y. W.; Lin, T. T.; Tjiu, W. W.; He, C. Tuning self-assembly of hybrid PLA-P(MA-POSS) block copolymers in solution via stereocomplexation. *Polym. Chem.* **2013**, *4* (4), 1250−1259.
(33) Tsuji, H.; Horii, F.; Hyon, S. H.; Ikada, Y. Stereocomplex formation between enantiomeric poly(lactic acid)s. 2. Stereocomplex formation in concentrated solutions. *Macromolecules* **1991**, *24* (10), 2719−2724.
(34) Bouapao, L.; Tsuji, H. Stereocomplex crystallization and spherulite growth of low molecular weight poly(L-lactide) and poly(D-lactide) from the melt. *Macromol. Chem. Phys.* **2009**, *210* (12), 993−1002.
(35) Biela, T.; Duda, A.; Penczek, S. Enhanced melt stability of star-shaped stereocomplexes as compared with linear stereocomplexes. *Macromolecules* **2006**, *39* (11), 3710−3713.
(36) Brzeziński, M.; Bogusławska, M.; Ilčíková, M.; Mosnáček, J.; Biela, T. Unusual thermal properties of polylactides and polylactide stereocomplexes containing polylactide-functionalized multi-walled carbon nanotubes. *Macromolecules* **2012**, *45* (21), 8714−8721.
(37) Xu, H.; Xie, L.; Chen, Y. H.; Huang, H. D.; Xu, J. Z.; Zhong, G. J.; Hsiao, B. S.; Li, Z. M. Strong shear flow-driven simultaneous formation of classic shish-kebab, hybrid shish-kebab, and trans-crystallinity in poly(lactic acid)/natural fiber biocomposites. *ACS Sustainable Chem. Eng.* **2013**, *1* (12), 1619−1629.
(38) Zhong, Y.; Fang, H. G.; Zhang, Y. Q.; Wang, Z. K.; Yang, J. J.; Wang, Z. G. Rheologically determined critical shear rates for shear-induced nucleation rate enhancements of poly(lactic acid). *ACS Sustainable Chem. Eng.* **2013**, *1* (6), 663−672.
(39) Rasal, R. M.; Janorkar, A. V.; Hirt, D. E. Poly(lactic acid) modifications. *Prog. Polym. Sci.* **2010**, *35* (3), 338−356.
(40) Lai, W.-C.; Liau, W.-B.; Lin, T.-T. The effect of end groups of PEG on the crystallization behaviors of binary crystalline polymer blends PEG/PLLA. *Polymer* **2004**, *45* (9), 3073−3080.
(41) Kulinski, Z.; Piorkowska, E. Crystallization, structure and properties of plasticized poly(L-lactide). *Polymer* **2005**, *46* (23), 10290−10300.
(42) Kulinski, Z.; Piorkowska, E.; Gadzinowska, K.; Stasiak, M. Plasticization of poly(L-lactide) with poly(propylene glycol). *Biomacromolecules* **2006**, *7* (7), 2128−2135.
(43) Li, H.; Huneault, M. A. Effect of nucleation and plasticization on the crystallization of poly(lactic acid). *Polymer* **2007**, *48* (23), 6855−6866.
(44) Yang, C.-F.; Huang, Y.-F.; Ruan, J.; Su, A.-C. Extensive development of precursory helical pairs prior to formation of stereocomplex crystals in racemic polylactide melt mixture. *Macromolecules* **2012**, *45* (2), 872−878.
(45) Hoogsteen, W.; Postema, A. R.; Pennings, A. J.; Ten Brinke, G.; Zugenmaier, P. Crystal structure, conformation and morphology of solution-spun poly(L-lactide) fibers. *Macromolecules* **1990**, *23* (2), 634−642.
(46) Pan, P.; Kai, W.; Zhu, B.; Dong, T.; Inoue, Y. Polymorphous crystallization and multiple melting behavior of poly(L-lactide): Molecular weight dependence. *Macromolecules* **2007**, *40* (19), 6898−6905.
(47) Pan, P.; Liang, Z.; Zhu, B.; Dong, T.; Inoue, Y. Roles of physical aging on crystallization kinetics and induction period of poly(L-lactide). *Macromolecules* **2008**, *41* (21), 8011−8019.
(48) Zhang, J.; Tashiro, K.; Tsuji, H.; Domb, A. J. Disorder-to-order phase transition and multiple melting behavior of poly(L-lactide) investigated by simultaneous measurements of WAXD and DSC. *Macromolecules* **2008**, *41* (4), 1352−1357.
(49) Rahman, N.; Kawai, T.; Matsuba, G.; Nishida, K.; Kanaya, T.; Watanabe, H.; Okamoto, H.; Kato, M.; Usuki, A.; Matsuda, M.; et al. Effect of polylactide stereocomplex on the crystallization behavior of poly(L-lactic acid). *Macromolecules* **2009**, *42* (13), 4739−4745.
(50) Zhang, Y.; Wang, Z.; Jiang, F.; Bai, J.; Wang, Z. Effect of miscibility on spherulitic growth rate for double-layer polymer films. *Soft Matter* **2013**, *9* (24), 5771−5778.
(51) Tsuji, H.; Hyon, S. H.; Ikada, Y. Stereocomplex formation between enantiomeric poly(lactic acid)s. 3. Calorimetric studies on blend films cast from dilute solution. *Macromolecules* **1991**, *24* (20), 5651−5656.